molecular pharmaceutics

ARTICLE

pubs.acs.org/molecularpharmaceutics

In Vitro Primary Human and Animal Cell-Based Blood–Brain Barrier Models as a Screening Tool in Drug Discovery

Olivier Lacombe,[†] Orianne Videau,[‡] Delphine Chevillon,[†] Anne-Cécile Guyot,[‡] Christelle Contreras,[†] Sandrine Blondel,[‡] Laurence Nicolas,[†] Aurélie Ghettas,[‡] Henri Bénech,[‡] Etienne Thevenot,[§] Alain Pruvost,[‡] Sébastien Bolze,[†] Lucie Krzaczkowski,[‡] Colette Prévost,[†] and Aloïse Mabondzo*[,‡]

[†]Laboratoires Fournier S.A., Daix, France

[‡]CEA, DSV, iBiTecS, Service de Pharmacologie et d'ImmunoAnalyse, Groupe de Neuropharmacologie et Médicaments, Gif-sur-Yvette, France

[§]CEA, LIST, Sensors and Signal Processing Unit, F-91191 Gif-sur-Yvette, France

ABSTRACT: Brain penetration is characterized by its extent and rate and is influenced by drug physicochemical properties, plasma exposure, plasma and brain protein binding and BBB permeability. This raises questions related to physiology, interspecies differences and *in vitro*/*in vivo* extrapolation. We herein discuss the use of *in vitro* human and animal BBB model as a tool to improve CNS compound selection. These cell-based BBB models are characterized by low paracellular permeation, well-developed tight junctions and functional efflux transporters. A study of twenty drugs shows similar compound ranking between rat and human models although with a 2-fold higher permeability in rat. cLogP < 5, PSA < 120 Å, MW < 450 were confirmed as essential for CNS drugs. An *in vitro*/*in vivo* correlation in rat (R^2 = 0.67; $P = 2 \times 10^{-4}$) was highlighted when *in vitro* permeability and efflux were considered together with plasma exposure and free fraction. The cell-based BBB model is suitable to optimize CNS-drug selection, to study interspecies differences and then to support human brain exposure prediction.

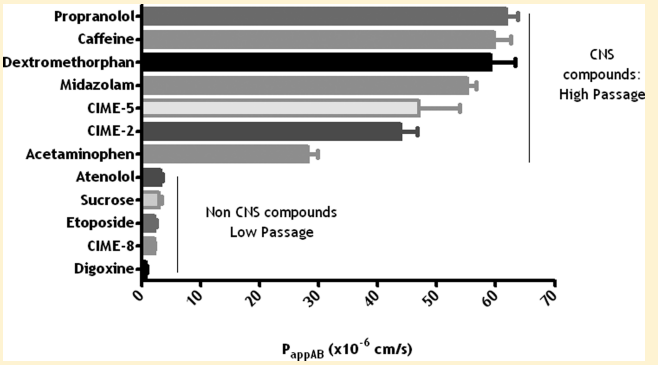

KEYWORDS: drug transport study, in vitro cell-based rat and human blood–brain barrier models, *in vivo*–*in vitro* correlation, plasma and brain free fraction, interspecies differences

INTRODUCTION

Lack of efficacy and unexpected toxicity are the major causes of drug failure in clinical trials. If preclinical activities are to allow a high quality drug candidate selection, complexities surrounding the drug candidate properties with respect to pharmacological efficacy, pharmacokinetics or safety need to be thoroughly investigated in order to enable extrapolation from animal to human. Within this context of interspecies extrapolation, a prime determinant is the manner in which drugs penetrate biological barriers such as the cell membrane, intestinal wall or blood–brain barrier (BBB). This is especially true for drug candidates designed to be active on a target located in the central nervous system (CNS) and which have to first cross the gut membrane if administered orally and then the BBB before reaching their target. Therefore it is unlikely that *in vitro* efficacy alone, without the properties necessary to penetrate the BBB, will result in *in vivo* efficacy in patients. Moreover, pharmacological potency in animals does not guarantee a similar potency in human at the equivalent dose because of a relatively lower human BBB permeability rate or extent when compared to animals.

Thus, given the exorbitant cost of new drug development,[1] it would be highly desirable to have physiologically relevant and cost efficient *in vitro* high-throughput tools to estimate BBB permeation before proceeding with expensive and time-consuming animal brain/plasma studies or, worse yet, to clinical trials with compounds with unknown human brain penetration. With such tools, for example, pharmacologically promising drug candidates without an effective BBB permeation would be rapidly excluded, then chemically modified to improve their intrinsic permeability by removing structural features that mediate interaction(s) with efflux proteins[2−6] and/or lowering binding to brain tissue.[7]

Indeed, brain penetration relies on drug physicochemical properties and several pharmacokinetic properties, including plasma exposure, plasma and brain protein binding and intrinsic BBB permeability.[8−10] Physicochemical properties, plasma pharmacokinetics, and more recently the plasma and brain free fractions are commonly used in discovery phases with reliable experiments or widely accepted calculations.

Regarding the free fraction determination in plasma and brain tissue, literature highlights the major importance of drug concentration in brain and plasma tissues for cross-correlating

Received: May 29, 2010
Accepted: March 27, 2011
Published: March 27, 2011

Table 1. Summary of the Physicochemical Properties, AUC_{brain}, AUC_{plasma}, Free Fraction in Plasma and Brain Tissues, Apparent Permeability from Apical to Basal Compartment (P_{appAB}) and Efflux Ratio Measured with the *in Vitro* Rat and Human Cell-Based BBB Models for the 20 Selected Compounds

							in vitro P_{appAB} ($\times 10^6$ cm/s)		AUC (μM h)		free fractions		ratios	
compd	MW	cLogP	PSA	HD	RB	HA	human (ER[a])	rat (ER)	plasma	brain	plasma	brain	AUC_{brain}/AUC_{plasma}	$f_{u,plasma}/f_{u,brain}$
SLV1	443	1.04	117	8	3	4	4.85 (1.5)	8.22 (1)	34.3	4.8	0.09	0.39	0.14	0.23
SLV2	619	8.2	50	4	1	13	0.64 (2.1)	0.85 (3)	14.1	4.2	0.04	0.01	0.30	7.40
SLV3	568	6.17	85	5	1	7	nv[b]	nv	16	13.9	0.01	0.01	0.87	2.80
SLV4	481	4.82	66	4	1	6	15.22 (1.6)	61.13 (0.4)	18.1	25.4	0.02	0.01	1.40	2.18
SLV5	233	2.64	78	4	2	3	24.65 (0.9)	33.55 (5.67)	19	98.4	0.07	0.1	5.19	0.73
SLV6	561	2.49	80	7	2	13	1.89 (9.8)	7.65 (3.5)	0.12	0.04	0.13	0.11	0.30	1.23
SLV7	408	3.89	50	6	1	6	31.02 (1.2)	20.61 (1.4)	1.03	7.01	0.01	0.02	6.80	0.65
SLV8	349	0.92	109	7	3	4	26.76 (1)	30.94 (1.1)	1.14	0.11	0.18	1	0.1	0.18
SLV9	496	6.56	75	5	1	5	5.94 (1.6)	11.3 (1.2)	2.35	8.46	0.01	0.01	3.6	2.20
caffeine	194	−0.13	54	6	0	0	35.80 (1)	53.4 (0.5)	24.9	9	0.68	1	0.36	0.68
acetaminophen	151	0.34	49	2	2	3	9.79 (0.9)	25.28 (0.8)	2.41	1.37	0.3	0.96	0.57	0.32
phenacetin	151	1.09	49	2	1	2	nd[c]	47.08 (1)	1.8	4.99	0.35	0.87	2.78	0.41
midazolam	325	3.93	25	0	1	3	28.21 (1.5)	49.46 (0.9)	0.56	1.96	0.01	0.11	3.50	0.06
omeprazole	345	2.17	96	1	5	6	nv	nv	1.44	0.01	0.04	0.61	0.01	0.07
dextrometorphan	370	4.11	12	2	0	1	28.04 (1.5)	52.89 (0.8)	0.21	5.49	0.37	0.14	25.60	2.65
CIME-2 (amodiaquine)	356	4.77	48				17.97 (1.7)	39.3 (0.8)	0.19	4.71	0.04	0.13	24.8	0.29
tolbutamide	270	2.34	84	4	2	7	nv	nv	279	0.14	0.01	0.95	0	0.01
digoxin	781	0.85	203	5	2	4	0.21 (5.2)	0.95 (12)	1.44	0.75	0.68	0.44	0.52	1.53
CIME-8 (rosuvastatine)	481	0.42	149	14	6	13	1.89 (0.6)	6 (0.5)	0.11	0	0.01	0.95	0.03	0.01
CIME-5 (memantine)	179			9	3	12	26.31 (1.2)	42 (1.1)	0.79	50.1	0.34	0.25	63.80	1.37

[a] Efflux ratio. [b] Not validated experiment. [c] Not determined.

in vitro and *in vivo* pharmacokinetic data.[7,11−13] Only the free fraction in plasma is available to the BBB in order to reach the brain, and essentially free drug concentration in the brain was described to provide the pharmacological activity. However, the *in vivo* measurement of BBB penetration is time-consuming and expensive and uses numerous animals. A reduction in animal experiments is desirable on ethical grounds, in addition to more relevant screening tools for CNS drug candidate selection. Within that context, the development of relevant *in vitro* cell-based BBB models, which can better predict BBB permeability of drug candidates in the species studied, would allow significant improvements in research screening flow schemes. Up to now in discovery, the study of BBB permeability to screen CNS drug candidates with respect to membrane permeability has conventionally used available models such as Caco-2 and MDCK cells overexpressing human P-gp (MDCK-MDR1).[14−17] However, the membrane properties of those models are significantly different from those of the BBB, either in human or in animals, and usually the *in vivo* brain/plasma ratio remains the pivotal experiment to provide the compound brain penetration.[18−20] The physiological and pharmacological relevance of the BBB and its high complexity have led to the development of several *in vitro* models[21−24]designed to study cerebral permeation of CNS drugs. Among the limitations of these models are their high paracellular permeability and the absence of cell polarity, the latter being the main characteristic of *in vivo* brain endothelial cells.

On the whole, there is a significant unmet need for a physiologically relevant and predictive *in vitro* BBB model that could be used in discovery for assessing the BBB permeability of CNS-targeted compounds in animals (preclinical pharmacology models) and in human.

In the present study, we report the evaluation of a new *in vitro* cell-based BBB model, which was developed from a coculture of endothelial and glial cells from animal or human brains. This model was characterized by low paracellular permeability, optimal behavior of tight junctions and expression and activity of efflux transporters. A data set of twenty compounds, selected for their chemically diverse structures and affinity to efflux transporters, was used to establish the interest of *in vitro* cell-based BBB model as a screening tool in drug discovery. The BBB permeability was evaluated for all compounds both *in vitro,* using these primary rat and human[25] cell-based BBB models, and *in vivo,* using brain/plasma ratio in rat. Moreover, compound physicochemical properties [molecular weight (MW), LogP, polar surface area (PSA), H-donors and acceptors, RotBonds] were calculated, and the free fraction in plasma as well as in brain tissue was measured and their relevance evaluated.

EXPERIMENTAL SECTION

Animal Use and Assurances. Animal experiments are conducted in full compliance with local, national, ethical, and regulatory principles and local licensing regulations, per the spirit of Association for Assessment and Accreditation of Laboratory Animal Care. The animal studies were carried out in accordance with decree 87-848, issued on October 19, 1987, concerning animal experimentation in France, in an approved facility (accreditation No. A91505) and by workers with Ministry of Agriculture authorization, as specified in the decree.

Selection of Compounds. Twenty compounds [eleven CIME substrates (cocktail of substrates addressing the main of enzymes of drug metabolism and pharmacokinetic) and nine

Laboratoires Fournier compounds] were selected for their diverse chemical properties, all being substrates of cytochrome (CYP) or efflux transporters, and including CNS and non-CNS drugs. The CIME substrates were acetaminophen, midazolam, dextromethorphan, tolbutamide, CIME-2 (amodiaquin), CIME-5 (memantine), caffeine, digoxin, phenacetine, omeprazole and CIME-8 (rosuvastatin). Acetaminophen, midazolam, dextromethorphan, tolbutamide, CIME-2 and CIME-5 were purchased from Sigma-Aldrich (St. Louis, MO, USA); caffeine, digoxin and phenacetine were obtained from Fluka-Sigma Aldrich, and CIME-8 substrate was obtained from Toronto Research Chemicals (North York, Canada).

SLV1 to -9 were available from Laboratoires Fournier S.A. For all compounds physicochemical properties (molecular weight (MW), LogP, polar surface area (PSA), H-donors and acceptors, RotBonds) are included in Table 1.

Internal standards (meloxicam, pravastatine, lansoprazole and levallorphan) were purchased from Sigma-Aldrich (St. Louis, MO, USA). [$^2H_3$]-Acetaminophen glucuronide, [$^{13}C_3$]-1-hydroxymidazolam, [$^2H_3$]-omeprazole sulfone, [$^2H_{10}$]-CIME-2 and [$^2H_3$]-CIME-2M were purchased from different suppliers as described in the labeled materials section. All tested compounds (synthesized and purchased) had a purity of at least 95%.

Physicochemical Properties of Test Compounds. The physicochemical properties of the test compounds (MW, LogP, PSA), H-donors and acceptors, RotBonds) were calculated using the Advanced Chemistry development (ACD)/Laboratories version 8 software.

Labeled Materials. [U-^{14}C]-Sucrose (601 mCi mmol^{-1}), [^{3}H]-propranolol (24 Ci mmol^{-1}), and [^{3}H]- vinblastine (10.3 Ci mmol^{-1}) were purchased from Amersham (Buckinghamshire, U.K.). [$^2H_3$]-Acetaminophen glucuronide and [$^{13}C_3$]-1-hydroxymidazolam were purchased from Toronto Research Chemicals (North York, Canada). [$^2H_3$]-Omeprazole sulfone was obtained from @rtMolecule (Poitiers, France). [$^2H_{10}$]-CIME-2 was purchased from Medical Isotopes (Pelham, NH, USA). [$^2H_3$]-CIME-2M was obtained from BD Biosciences (Woburn, MA, USA).

***In Vitro* Cell-Based Rat and Human BBB Models.** *Brain Microvessel Preparation and Cell Culture.* Microvessels were isolated from brain samples after 1.5 h digestion with collagenase/Dispase (1 mg/mL, Roche, France) containing DNase 1 (20 units/mL, Roche, France), followed by a 20% BSA gradient as described elsewhere.[26] The resulting microvessels obtained in the pellet were further digested with collagenase-Dispase (1 mg/mL, Roche, France) containing DNase 1 (20 units/mL, Roche, France) for 1 h at 37 °C while the supernatant containing a layer of myelin was centrifuged, washed and cultured in 75 cm^2 in the glial specific medium supplemented with 10 μg mL^{-1}, hEGF, 10 mg mL^{-1} insulin, 25 μg mL^{-1} progesterone, 50 mg mL^{-1} transferrin, 50 mg mL^{-1} gentamicin, 50 μg mL^{-1} 1% amphotericin B, 1% of human serum and 5% of fetal bovine serum.

Microvessel endothelial cells clusters after collagenase-Dispase digestion were passed through a 20 μm nylon mesh. The microvessels retained by the nylon mesh were collected and washed.

For RNA isolation and real-time PCR experments, the purity of collected brain microvessels were checked by measuring the expression of cell specific marker genes using specific primer for brain endothelial cells (CD31 or PECAM), for glial cells (Glial fibrillary acid protein or GFAP) and for pericytes (α-actin).

For brain endothelial isolation, isolated brain microvessels were cultured in 25 cm^2 flask coated with collagen type IV and fibronectin (0.1 mg/mL) in the presence of puromycine (2 μg/mL) in the endothelial basal medium containing 0.1% human recombinant epidermal growth factor (hEGF), 0.04% hydrocortisone, 0.1% human recombinat insulin like growth factor, 0.1% ascorbic acid, 0.1% gentamin, 0.1% amphotericin-BN and 5% fetal bovine serum. On the third day, the cells received a new endothelial specific medium without puromycine. When cells reached confluence (70%) at day 7, the purified endothelial cells were frozen and ready to be used for *in vitro* cell-based BBB genesis and drug transport experiments.

Cell-Based Blood−Brain Barrier Model. Glial cells (2×10^4 cells) were plated on Transwell plates (Costar, pore size 0.4 μm; diameter 12 mm; insert growth area 1.12 cm^2, Dutscher SA, Brumath, France) in a glial specific medium (α-MEM/F12) supplemented with 10 μg mL^{-1}, hEGF, 10 mg mL^{-1} insulin, 25 μg mL^{-1} progesterone, 50 mg mL^{-1} transferrin, 50 mg mL^{-1} gentamicin, 50 μg mL^{-1} 1% amphotericin B, 1% of human serum and 5% of fetal bovine serum. After 24−72 h, BECs (5×10^4 cells) were plated on the upper side of a collagen-coated polyester Transwell membrane (Costar, pore size 0.4 μm; diameter 12 mm; insert growth area 1 cm^2) in 0.5 mL of the endothelial basal medium-2 (EBM-2, LONZA, Walkersville, MD, USA) containing 0.1% human recombinant epidermal growth factor (hEGF), 0.04% hydrocortisone, 0.1% human recombinat insuline like growth factor, 0.1% ascorbic acid, 0.1% gentamin, 0.1% amphotericin-BN and 5% fetal bovine serum. (0.5 mL). The chambers containing human glial cells and BECs were considered as the basolateral and apical compartment, respectively. The microplates were then incubated at 37 °C in a 5% CO_2 atmosphere. Under these experimental conditions, BECs formed a confluent monolayer within 15 days.

Checking the Integrity of the Cell-Based BBB Models. The integrity of the cell-based BBB models was demonstrated (i) by assessing the presence of tight junctions between the endothelial cells under a confocal microscope, mRNA transcriptional profiles and (ii) by measuring the flux of the paracellular reference marker, [^{14}C]-sucrose, through the monolayer.

For immunostaining, BEC monolayers were fixed with cytofix-cytoperm buffer (Pharmigen, France) and permeabilized with Perm/Wash buffer (Pharmigen) according to the manufacturer's procedure. The samples were washed with PBS and soaked in the blocking solution containing 4% BSA. They were then incubated with the rabbit anti-Zonula occuldens (ZO-1), rabbit anticlaudin-3 and mouse anticlaudin-5 mAb from Zymed laboratories (San Francisco, CA). After washing, the cells were incubated with the secondary FITC antibody (Becton-Dickinson, San Diego, CA). The preparations were examined with a fluorescence microscope.

The BBB integrity was checked by assessment of sucrose permeability as a marker to validate the experiments before and after test compound incubations. Before use of the monolayers, BBB integrity was checked on 12% of monolayers. Transwells with HBMEC monolayers were transferred to new plates. T buffer (150 mM NaCl, 5.2 mM KCl, 2.2 mM $CaCl_2$, 0.2 mM $MgCl_2$, 6 mM $NaHCO_3$, 2.8 mM glucose and 5 mM Hepes) was added: 1.5 mL to the basolateral compartment (B) and 0.5 mL to the apical compartment (A), which also contained 0.37×10^{10} Bq/mL of [^{14}C]-labeled sucrose. After 60 min of incubation at 37 °C, supernatants from both A and B compartments were collected and the amount of tracer that passed through the endothelial monolayer was determined by scintillation counting. Monolayers were validated for sucrose permeability from A to B and B to A below 8×10^{-6} cm s^{-1}.

Transcription Profiles of Tight Junctions, Efflux Transporters and Other Receptors. For a thorough evaluation of the *in vitro* cell-based rat BBB model, the mRNA expression profiles of tight junctions (Claudine-5, ZO-1) and ABC transporters (abcb1, abcc1, abcc2, abcc4, abcc6, abcbg2) were assessed as previously described. RNA was isolated using GenEluteTM mammalian total RNA kit (Sigma, Aldrich). Total RNA concentration and purity were then determined by measuring absorbance at 260 and 280 nm. The A260/280 ratio ranged between 1.8 and 2.

A sample of 0.5 μg of total RNA was converted to cDNA with random primers in a total volume of 10 μL using RT^2 first strand kit (Superarray Bioscience Corporation, USA). The cDNA was diluted with distilled water to a volume of 100 μL. 0.4 μM was used for each primer set in a specific RT^2 profiler PCR array according to the manufacturer's protocol. Relative expression values were calculated as $2^{-\Delta CT}$, where ΔCT is the difference between the amplification curve (CT) values for genes of interest and the housekeeping gene (hypoxanthine-guanine phosphoribosyltransferase, HPRT). If the CT was higher than 35, we considered the expression level too low to be applicable.

In Vitro Drug Transport Study. After checking BBB integrity, Transwells with BEC monolayers were transferred to new plates. T buffer (150 mM NaCl, 5.2 mM KCl, 2.2 mM $CaCl_2$, 0.2 mM $MgCl_2$, 6 mM $NaHCO_3$, 2.8 mM glucose and 5 mM Hepes) was added: 1.5 mL to the basal chamber (B) and 0.5 mL to the apical chamber (A). Experiments were performed in triplicate for each compound. The compounds (10 μM) were introduced in the donor chamber (either the apical or the basal compartment). After 60 min, aliquots were removed from the acceptor and basal chambers for drug-concentration determination as previously described.[26]

The P_{app} value was calculated as followed:

$$P_{app} = dQ/dT \times A \times C_0 \quad (1)$$

where dQ/dT is the amount of drug transported per time point; A is the membrane surface area; and C_0 is the donor concentration at time point 0. Data are presented as the average ± SD from three monolayers. Mass balance of all compounds was between 80% and 120%.

The mass balance was calculated as follows:

$$R\ (\%) = ([(A_p + B_s)/A_0] \times 100 \quad (2)$$

where A_p and B_s are the amount of tested compounds in the apical and basal compartments, respectively. A_0 is the initial amount in the donor compartment at time point 0.

***In Vivo* Experiments.** *Time Course Distribution Study of Drug in Plasma and Brain of Rat.* The study was conducted in accordance with protocols laid down by the Laboratoires Fournier Animal Welfare policy. The *in vivo* plasma and brain exposure to tested compounds was assessed after oral gavage (SLV compounds) or 3 min intravenous infusion (CIME compounds) in the male Wistar rat (300−350 g, IFFA Credo, France). For oral gavage, compounds were administered at 10 mg/kg by gavage as suspension in methycellulose 400 cP 1%. For intravenous infusion, the animals were anesthetized (isofurane/oxygen 5% for induction and 3% thereafter) and catheterized in the tail vein before a 3 min infusion of the test compound solution at 1 mg/kg.

Two rats per time point were used, up to 24 h postdosing. Blood was sampled from the retro-orbital sinus in Eppendorf tubes containing 20 μL of a sodium heparinate evaporated solution at 1000 U/mL^{-1} and then centrifuged for 5 min at 3000*g* at 4 °C to collect plasma. After collection, brains were weighed and then frozen in liquid nitrogen. Plasma samples and brains were subsequently stored at −20 °C until bioanalysis

Experimental Assessment of Plasma and Brain Protein Binding. The *in vitro* rat plasma and brain protein binding was assessed for each tested compound at 10 μM (0.5% DMSO). Plasma protein binding was determined by ultracentrifugation (4 h at 400000*g*) and brain protein binding by equilibrium dialysis with a 96-well plate system (brain homogenate ∼25 mg mL^{-1} protein, equilibrium time 6 h). Recoveries were >75%, except for omeprazole (65%) and SLV2 (70%).

Bioanalysis of CIME Compounds. *Samples from in Vitro BBB Permeability Experiments.* CIME cocktail substrates were assayed *in vitro* BBB media using a LC−MS/MS method. In short, 20 μL of a solution mixture of internal standards, namely, lansoprazole, levallorphan, [$^2H_3$]-acetaminophen glucuronide, [$^{13}C_3$]-1-hydroxymidazolam, meloxicam, and [$^2H_{10}$]-CIME-2, was added to 200 μL of incubation medium, and samples were left to stand for 15 min. Finally, 20 μL was injected into the chromatographic system made up of an Acquity UPLC system coupled to a triple quadrupole mass spectrometer Quattro Premier XE equipped with a turbo spray ionization source (Waters, Saint Quentin en Yvelines, France). System control and data processing were carried out using MassLynx software version 4.1. The chromatographic step was performed on an ACQUITY UPLC BEH Shield RP18 column (2.1 mm × 100 mm, 1. 7 μm) coupled with a ACQUITY UPLC BEH Shield RP18 1.7 μm Van Guard Pre-Column (Waters, Saint Quentin en Yvelines, France) set at 50 °C. A gradient of two solvent mixtures was delivered at 0.4 mL/min. Solvent A comprised 0.1% formic acid in water and solvent B, 0.1% formic acid in acetonitrile. Analytes were ionized in either positive or negative mode (4-OH-tolbutamide and phenacetine). Tuning parameters were as follows: capillary voltage 3 kV, source temperature 120 °C, desolvatation temperature 350 °C, desolvatation nitrogen gas 900 L/h, cone gas 10 L/h, collision argon gas flow 0.05 mL/min with a pressure of 2.6 × 10^{-3} bar. Multiple reaction monitoring was used for analyte quantification against internal standards.

Plasma Samples. Five hundred micrograms of the internal standard mixture in 2% NH_4OH was spiked in 250 μL of rat plasma, and samples were allowed to stand for 15 min at room temperature. Then 1 mL of the mixture underwent solid phase extraction (SPE), i.e. loaded onto an Oasis MAX cartridge (30 mg, 1 cm^3) (Waters), which had previously been conditioned with 1 mL of methanol followed by 1 mL of water. Washing steps were performed with 1 mL of water and 1 mL of 5% methanol in water. Analytes were eluted with 2 × 250 μL of 2% formic acid in methanol and 2 × 250 μL of acetonitrile/methanol (1/1, v/v) in a polypropylene tube already containing 75 μL of 2% NH_4OH in 10 mM ammonium acetate. Using vortex mixing, eluates were evaporated to dryness (1 h, 40 °C) in a turbovap (Caliper). The dry residues were reconstituted in 100 μL of 10% methanol in 10 mM ammonium acetate, and, after vortex mixing, 20 μL was injected into the same chromatographic system as that used for *in vitro* experiments). The quantification was carried out using standard curves prepared from blank brain tissue spiked with CIME cocktail substrates and metabolites. The following internal standards were used: lansoprazole for omeprazole and metabolites, levallorphan for CIME-5, dextromethorphan and metabolites, [$^2H_3$]-acetaminophen glucuronide for digoxine, acetaminophen and metabolites, [$^{13}C_3$]-1-hydroxymidazolam for midazolam and

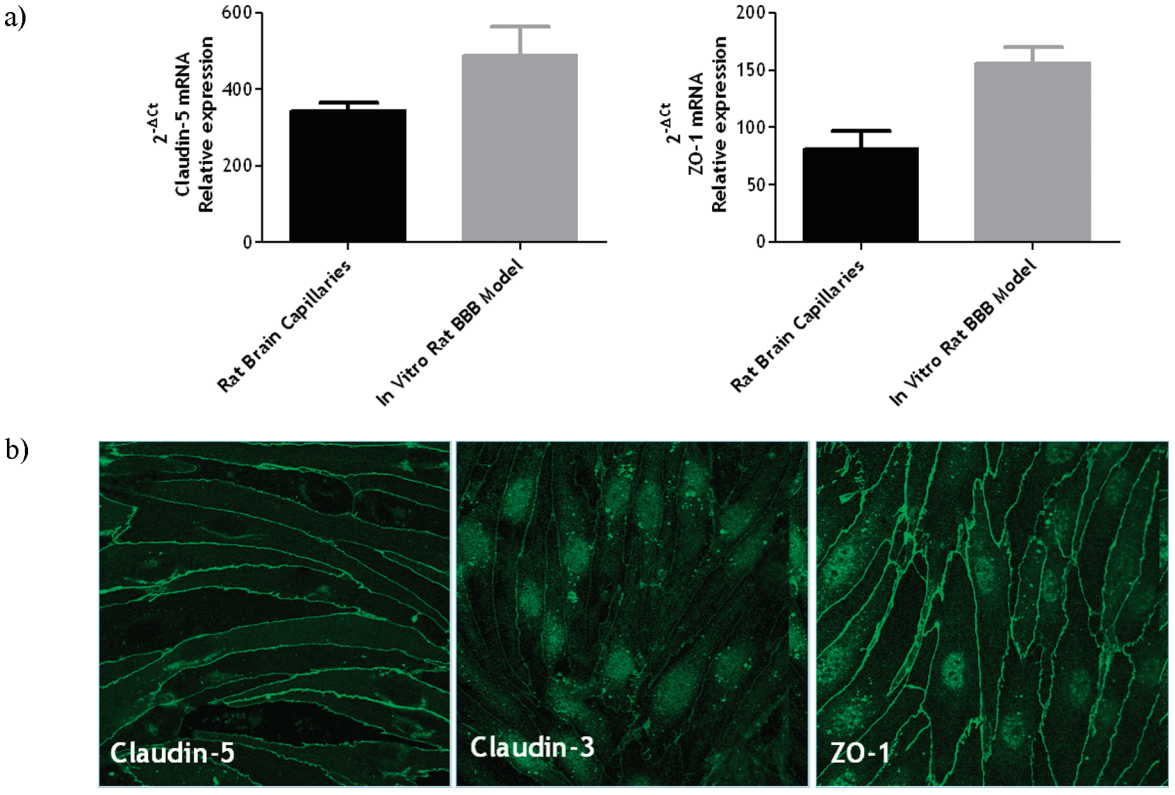

Figure 1. (a) Checking *in vitro* rat cell-based BBB model integrity. mRNA transcription profiles for claudin-5 and ZO-1 by semiquantitative RT-PCR performed in isolated brain endothelial microvessels from brain cortex, brain endothelial cells cultured above glial cells. Results are mean ± SD of 10 rat brain endothelial microvessels and a pool of 10 brain endothelial cells in duplicate. (b) Fluorescence photomicrographs: Primary rat brain endothelial cells stained for ZO-1, claudin 5 and claudin 3.

metabolites, [$^2H_3$]-omeprazole sulfone for omeprazole sulfone, meloxicam for phenacetin, tolbutamide and metabolites, pravastatin for CIME-8, [$^2H_3$]-CIME-2M for CIME-2M (corresponding metabolite of the CIME-2 substrate). Specificity, precision, accuracy, total recovery, dilution and stability during the process and in the autosampler were checked and fulfilled the recommended ranges.

Brain Samples. Rat brains were weighed and homogenized in ultrapure water (1/2, w/v) using an Ultraturax. One milliliter of the internal standards (see above) solution in methanol was added to 200 μL of brain homogenate. After centrifugation (10 min, 20000*g*, 4 °C, supernatants were evaporated to dryness (2 h, 40 °C) in a Turbovap (Caliper). Dry residues were resuspended in 500 μL of 1% NH_4OH and submitted to the same solid phase extraction as for plasma and the same LC−MS/MS method as for *in vitro* experiments (see above). Quantification was carried out using standard curves prepared from blank brain tissue spiked with CIME cocktail substrates and metabolites. The following internal standards were used: lansoprazole for omeprazole and metabolites, levallorphan for CIME-5, dextromethorphan and metabolites, [$^2H_3$]-acetaminophen glucuronide for phenacetine, acetaminophen and metabolites, [$^{13}C_3$]-1-hydroxymidazolam for midazolam and metabolites, [$^2H_3$]-omeprazole sulfone for omeprazole sulfone, pravastatin for CIME-8, [$^2H_3$]-CIME-2M for CIME-2M.

Bioanalysis of SLV Compounds. Sample preparation was adapted to all different samples: the *in vitro* samples (from BBB permeability experiments) were diluted with a mixture of blank matrix and acetonitrile; the plasma samples (from *in vivo* pharmacokinetics and from plasma protein binding assessment) and brain homogenates (from brain protein binding assessment) were analyzed after protein precipitation with organic solvents; the rat brain samples (from *in vivo* pharmacokinetics) were weighed and homogenized with a mixture of aqueous solution and organic solvents using the IKA grinder.

All samples were analyzed by LC−MS/MS using the multiple reaction monitoring mode specific to each analyte and to the internal standards. For the *in vitro* BBB samples, the LC−MS/MS system consisted of two pumps (1100, Agilent Technologies), a column oven (1100, Agilent Technologies), an HTS PAL autosampler (CTC Analytics) and a hybrid quadrupole linear ion trap mass spectrometer (API4000Qtrap, Applied Biosystems/MDS Sciex) with an ESI source. The analytical column was a Zorbax Eclipse XDB C18 (100 × 3 mm, 3.5 μm) (Agilent Technologies), the flow rate was 0.6 mL/min and the injection volume was 2 μL. For the protein binding samples or *in vivo* samples, the LC−MS/MS system consisted of an online degasser (DGU-20 A3, Shimadzu), two pumps (LC-20ADXR, Shimadzu), a column oven (CTO-20AC, Shimadzu), an autosampler (SIL-20ACXR), a system controller (CBM-20A, Shimadzu) and a hybrid quadrupole linear ion trap mass spectrometer (API4000Qtrap, Applied Biosystems/MDS Sciex) with an ESI source. The analytical column was an Acquity BEH (50 × 2.1 mm, 1.7 μm) (Waters), the flow rate was 0.8 mL/min and the injection volume was 2 μL.

Mass spectrometer conditions were optimized for each compound, since some were detected with the negative ionization mode and others with the positive ionization mode. For all tested compounds, a linear gradient of mobile phase A (ammonium

acetate 5 mM with 0.1% of acid formic) and mobile phase B (acetonitrile with 0.1% of acid formic) was optimized. An internal standard with the same ionization mode as the tested compound was added before sample preparation. Both the chromatrographic system and the mass spectrometer were controlled by Analyst software version 4.2. (API4000Qtrap, Applied Biosystems/MDS Sciex). Quantification was carried out using standard calibration curve and quality control samples prepared with blank matrix spiked with SLV compound.

Data Integration. The objectives of this work were first to evaluate the new human and rat cell-based BBB *in vitro* models as part of the drug discovery process, with a focus on interspecies differences and on the potential *in vitro*/*in vivo* correlation, with an aim toward subsequent human brain penetration prediction. Therefore, the comparison of *in vitro* permeability obtained with rat versus human cells was established. Moreover, considering that brain penetration depends on plasma exposure, plasma and brain protein binding and BBB permeability rate and extent,[7,11−13] we assessed a tentative relationship between all these combined parameters and brain exposure in rat. Second, as physicochemical properties have been well-described as impacting crossing of the BBB, their link to permeability results observed with the *in vitro* model was studied and compared to literature.[7]

Statistical Analysis. Statistical analysis was performed using the Prism 3.0 program (GraphPad Software, Inc., San Diego, CA) and the R statistical software (R Development Core Team, 2009). Regression lines were calculated and correlation was estimated by the two-tailed nonparametric Spearman test. A nonparametric two-tailed Mann−Whitney test was performed to assess the significant differences between different experimental conditions. Mean and SD were calculated. Statistical significance was set at $p < 0.05$.

RESULTS

***In Vitro* Primary Rat and Human Cell-Based Blood−Brain Barrier Models.** *Integrity, Inter- and Intraindividual Variability and Dynamic Range of Permeability of the in Vitro Cell-Based Human and Rat BBB Model.* The *in vitro* cell-based model of human BBB has been previously described,[25,26] thus we focus our study on the *in vitro* primary rat cell-based BBB model. We analyzed the transcriptional mRNA profile of claudin-5, ZO-1 involved in the tightness of BBB.

The expression level of claudin-5 and ZO-1 mRNA in *in vitro* primary rat cell-based BBB model was compared to that of freshly isolated brain endothelial microvessels. First of all, we evaluated the purity of brain endothelial microvessel preparation (isolated from a pool of 20 rat brain samples). PECAM-1 mRNA was the most expressed in brain microvessels (98.7 ± 0%) compared to GFAP (1 ± 0%) or α-actin (0.3 ± 0%) showing the acceptable purity of the rat brain microvessels.

Rat brain endothelial cell coculture on top of glial cells expresses mRNA for claudin-5, ZO-1 and claudin-3 (Figure 1a). The influence of glial cells on *in vitro* cell-based rat BBB properties was demonstrated by a trend to increased mRNA encoded for claudin-5 and ZO-1. To further demonstrate the presence of the corresponding proteins, immunostaining was performed. Rat brain endothelial cells express junction proteins such as claudin-5, claudin-3 and ZO-1. Figure 1b shows the continuous network of labeled claudin-3, claudin-5 and ZO-1 demonstrating that the *in vitro* primary brain endothelial monolayer displayed well-developed tight junctions in the *in vitro* primary rat cell-based BBB model. This integrity was associated

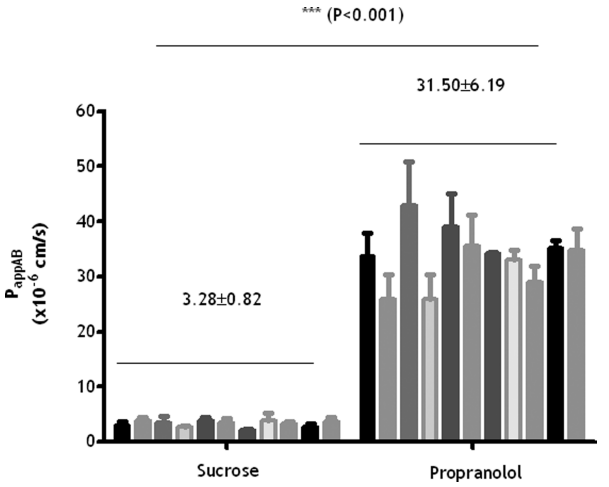

Figure 2. Low paracellular transport of sucrose and high permeability of propranolol from *in vitro* rat cell-based BBB model. Each batch represents a single batch of cells. Data are the mean of 11 different batches of cells in at least triplicate. ***, $p < 0.001$, a nonparametric Mann−Whitney test.

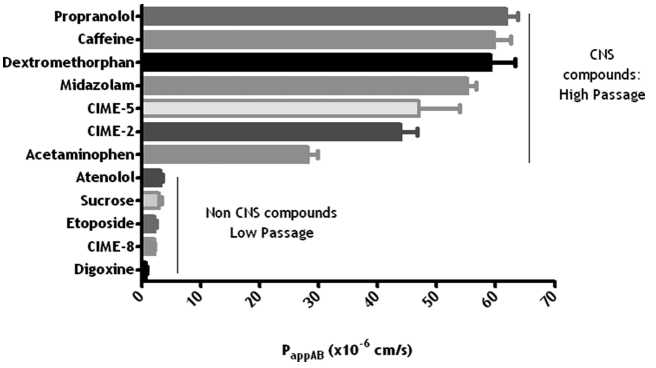

Figure 3. Permeability of CNS and non CNS compounds in *in vitro* rat cell-based BBB model. Data are the average of at least three cell monolayers for each test compound.

with a low paracellular permeability of sucrose across the brain endothelial cell monolayer. The mean P_{app} value of sucrose, a paracellular marker, on eleven different batches of cells in triplicate was 3.28 ± 0.82 cm s^{-1} × 10^{-6} (CV: 25%, $p < 0.001$) and by comparison to propranolol, a high BBB permeable marker, permeability (31.50 ± 6.19 × 10^{-6} cm s^{-1}; CV: 19.65%) indicated an overall restrictive paracellular permeation across the *in vitro* primary rat cell-based BBB model (Figure 2). The P_{app} value for sucrose in the *in vitro* rat cell-based BBB model is in the same range as in the *in vitro* primary human cell-based BBB: mean P_{app} value of sucrose from 9 different batches of 9 different donors was 2.69 ± 0.25 × 10^{-6} cm s^{-1} (CV: 23.28%).

Known CNS and non-CNS marketed drugs were used to assess permeability across the *in vitro* cell-based rat BBB model. The mean P_{app} value for the marketed non-CNS compounds from the apical to basal compartment was about 2.32 ± 0.93 × 10^{-6} cm s^{-1} (range: 0.87 × 10^{-6} cm s^{-1} to 3.27 × 10^{-6} cm s^{-1}), consistent with a limited passage across the rat brain endothelial cell monolayer. The mean P_{app} value for CNS compounds such as propranolol, midazolam, acetaminophen and phenacetin, consistent

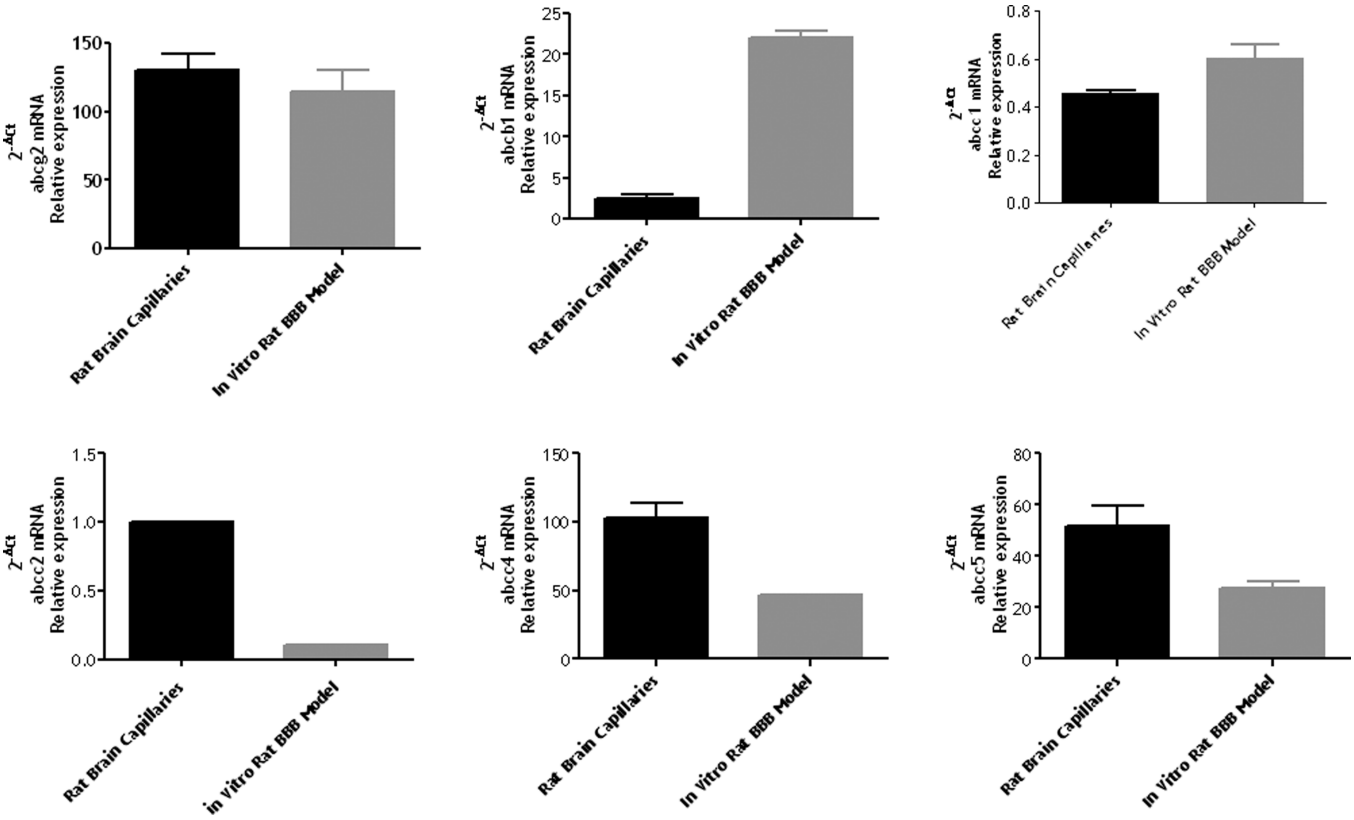

Figure 4. ABC transporter gene expression profile in rat brain microvessels and isolated brain endothelial cells cultured on top of glial cells. Results are mean ± SD of 10 rat brain endothelial microvessels and a pool of 10 brain endothelial cells in duplicate.

with high passive permeability, was about $50 \pm 11 \times 10^{-6}$ cm s^{-1} (Figure 3).

Transcription Profiles of Efflux Transporters and Other Transporters. The expression of six ABC transporters was investigated by semiquantitative RT-PCR in freshly isolated brain microvessels from brain cortex and in the corresponding isolated brain endothelial cell coculture on top of glial cells. Transcript levels for abcc1 and abcg2 in the *in vitro* cell-based rat BBB model were similar to those in freshly isolated pure brain endothelial microvessels, while mRNA expression of abcc4, abcc5, and abcc2 in *in vitro* cell-based rat BBB model decreases (Figure 4). mRNA transcripts for abcb1 in brain endothelial cells increased in the presence of glial cells, suggesting the role of glial cell factors in the regulation of abcb1 as described elsewhere.[27]

Selection of Compounds. Drugs selected cover a wider range of MW (range 151−781; mean 388), H donors (range 0−14; mean 5), H acceptors (range 0−13; mean 5.90), lipophilicity [(cLogP) range −0.13 to 8.2; mean 2.98], rotatable bonds (range 0−6; mean 1.95), and PSA (range 12.47−203; mean 77.89) as shown in Table 1. The *in vitro* cell-based rat BBB model demonstrated a large dynamic range, with P_{app} values spanning from 0.85×10^{-6} to 61.13×10^{-6} cm s^{-1} for the selected compounds.

***In Vitro* BBB Permeability versus Physicochemical Properties.** The relationships between *in vitro* apparent permeability using *in vitro* cell-based rat BBB model and physicochemical properties are summarized in Figure 5. No direct relationship was observed between *in vitro* BBB P_{app} and MW, cLogP, PSA (Figure 5), nor between H donors/acceptors and number of rotatable bonds (Table 1). However, compound physicochemical properties such as cLogP < 5, MW < 450 Da and PSA < 120 Å were confirmed to be favorable for a high BBB permeability as they were linked with high *in vitro* P_{app} values (from 20×10^{-6} cm s^{-1} to 60×10^{-6} cm s^{-1} using the *in vitro* primary rat cell-based BBB model) (Figure 5), and would be useful in the chemical design of new brain-targeting drug candidates.

In Vitro/in Vivo Correlation. Rat plasma and brain exposure to the test compounds are reported in Table 1.

Several recent publications focused on the impact of brain versus plasma protein binding and demonstrated that the protein binding ratio may reflect the brain penetration.[7,29] Good correlations were observed between the brain/plasma protein binding ratio and the *in vivo* brain/plasma AUC ratio. In the present study, even if no direct correlation was shown, the brain/plasma protein binding ratio allows exclusion of compounds with a low *in vivo* brain/plasma AUC ratio (Figure 6). In this case, the difference in protein binding would be the main factor involved in brain penetration and would go beyond the apparent permeability issues.[29] This relationship does not consider BBB permeability, which is assimilated as passive diffusion and does not take into account the potential active transporters present in the BBB. Nevertheless, BBB permeability may influence brain exposure since it is rate and extent limiting. The function of efflux-transporters as well as BBB permeability has been suggested to play a major role in the prediction of drug penetration in the brain.[7,28,30] In the present study, by collectively considering all factors that potentially impact brain exposure (plasma AUC, plasma and brain protein binding, BBB permeability rate and efflux ratio), a significant relationship was observed with the compounds with the undisclosed structure (R^2 = 0.67) (Figure 7A). On the whole

dx.doi.org/10.1021/mp1004614 |*Mol. Pharmaceutics* 2011, 8, 651–663

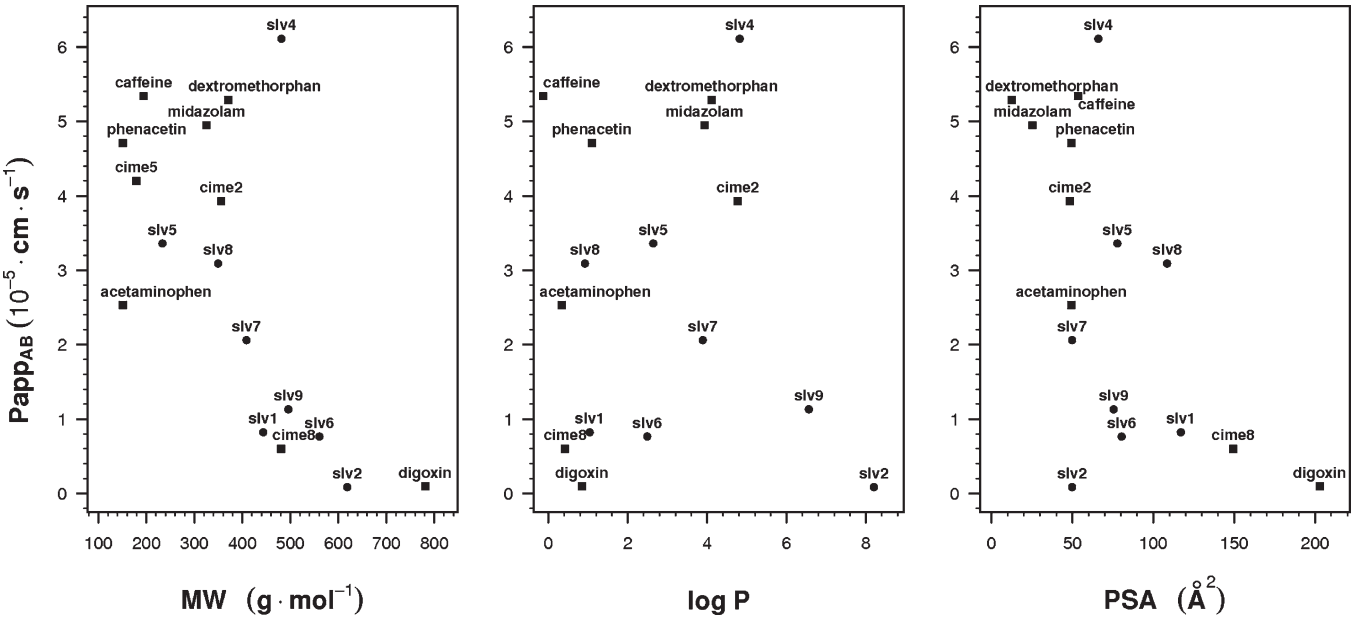

Figure 5. Relationship between molecular weight (MW), polar surface area (PSA), CLogp and apparent permeability (P_{app}) from *in vitro* rat cell-based BBB model. Filled circles: SLV set, Filled squares: CIME set.

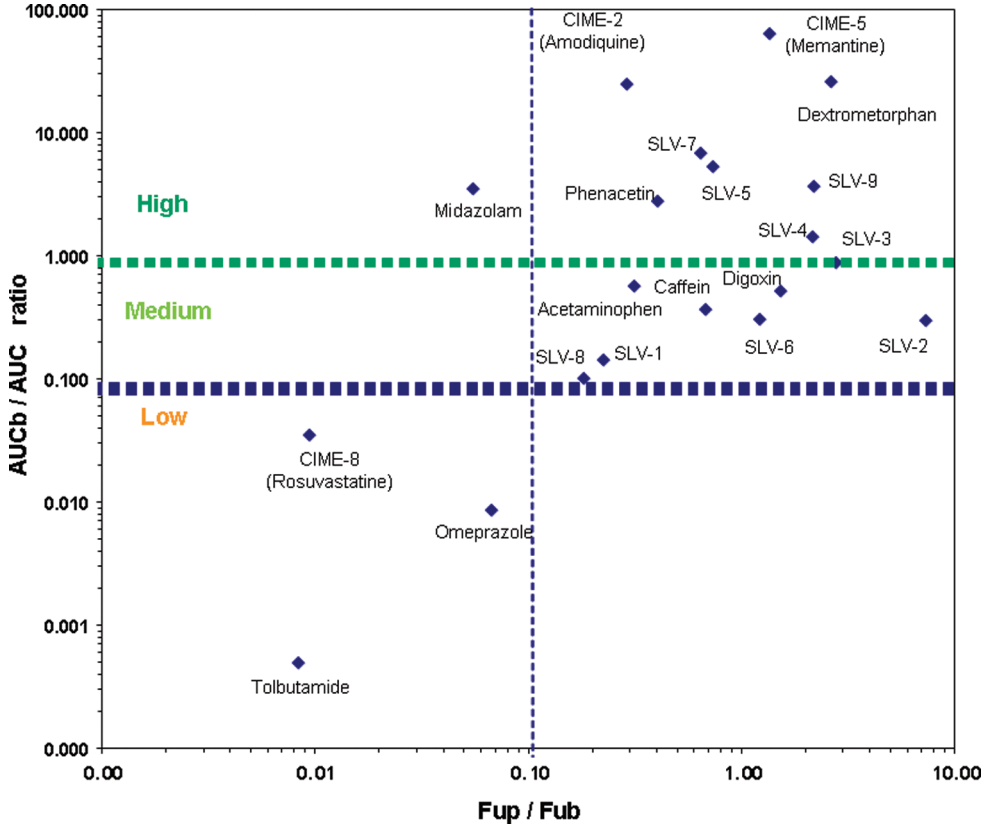

Figure 6. Relationship between BBB permeation *in vivo* in rat and unbound fraction in brain ($f_{u,brain}$) and plasma ($f_{u,plasma}$) tissues.

(compounds with disclosed and undisclosed structure), an interesting *in vitro*/*in vivo* correlation in rat BBB was observed ($R^2 = 0.67$, $P = 2 \times 10^{-4}$) (Figure 7B).

***In Vitro* Interspecies Differences in Rat vs Human.** Prior to using the *in vitro* primary rat and human cell-based BBB models, the tightness of the BEC monolayer was consistently checked by assessing the permeability of [^{14}C]-sucrose. The permeability of the selected compounds was then measured bidirectionally: apical to basal (P_{appAB}) and basal to apical compartments (P_{appBA}). The P_{appBA}/P_{appAB} efflux ratio (ER) was calculated.

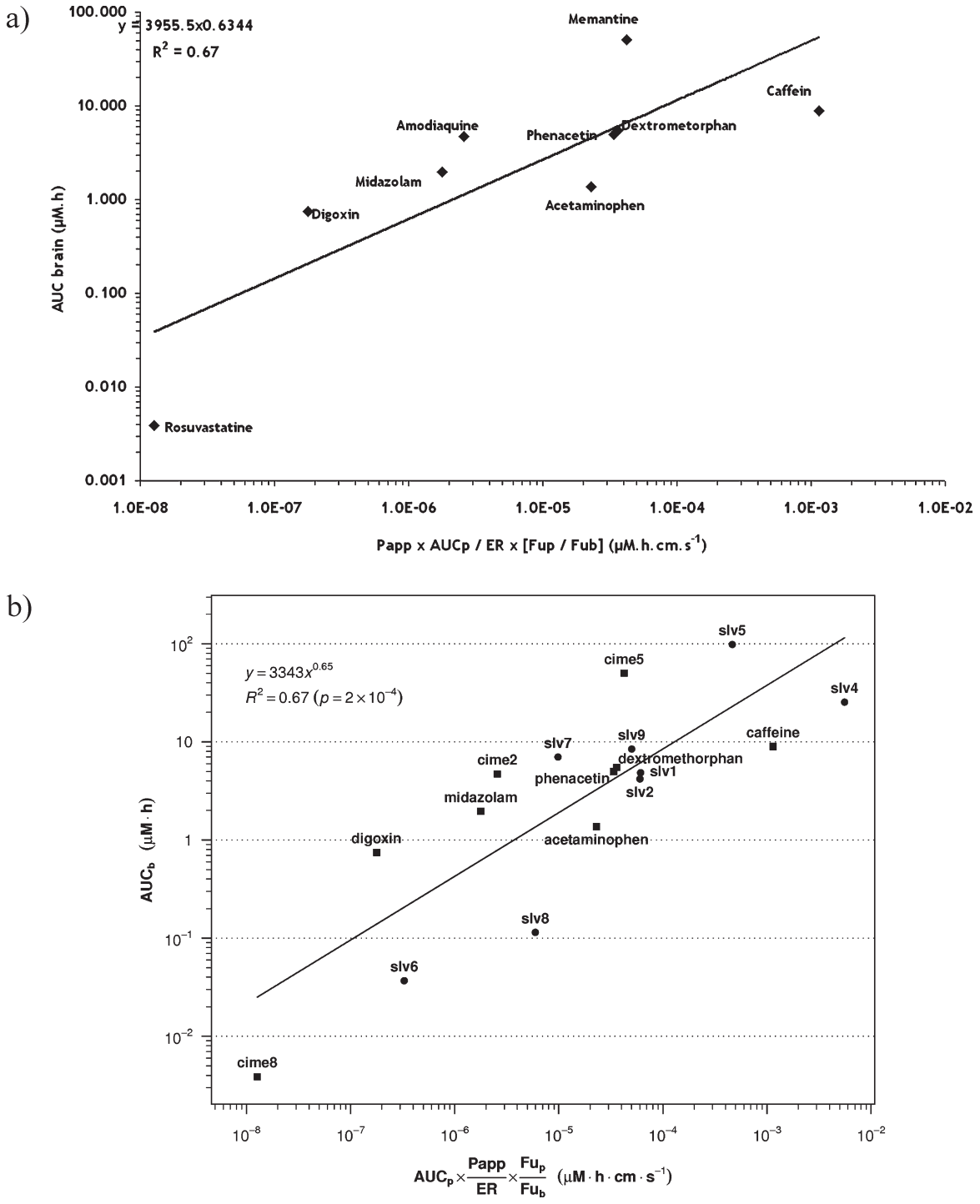

Figure 7. *In vitro*/*in vivo* correlation: *in vivo* brain distribution (AUC_{brain}) of selected compounds with respect to plasma distribution (AUC_{plasma}), *in vitro* passive permeability (P_{app}) from *in vitro* rat cell-based BBB model, *in vitro* efflux ratio and unbound fraction in plasma ($f_{u,plasma}$) and brain ($f_{u,brain}$) tissues. (a) Regression analysis with known CIME compounds ($R^2 = 0.67$). (b) Regression analysis with all sets of compounds: ($R^2 = 0.67$, $p = 2 \times 10^{-4}$).

Conventionally, compounds with a ER above 2 are considered to undergo active efflux, compounds with a ER below 0.5 are considered to undergo active uptake and compounds with a ER between 0.5 and 2 are considered to cross the BBB by passive diffusion.[25] In this study, compounds known to be efflux-transporter substrates in human such as digoxin and SLV6 (ER: 5.2 and 9.8, respectively) are likely to also be substrates in rat (ER: 12 and 3.5, respectively) (Table 1). Figure 8 reveals that there is a correlation between the two BBB models. However, the high correlation was observed with the known CIME compounds ($R^2 = 0.94$). Considering the whole data set, a trend of correlation ($R^2 = 0.61$) was observed between *in vitro* rat and human cell-based BBB models, broadly indicating a similar ranking of compounds between rat and human BBB models. Compounds (SLV4, -5, -7 and -8) may reflect a negative correlation mainly driven by the compounds SLV4 and -7. The

dx.doi.org/10.1021/mp1004614 |*Mol. Pharmaceutics* 2011, 8, 651–663

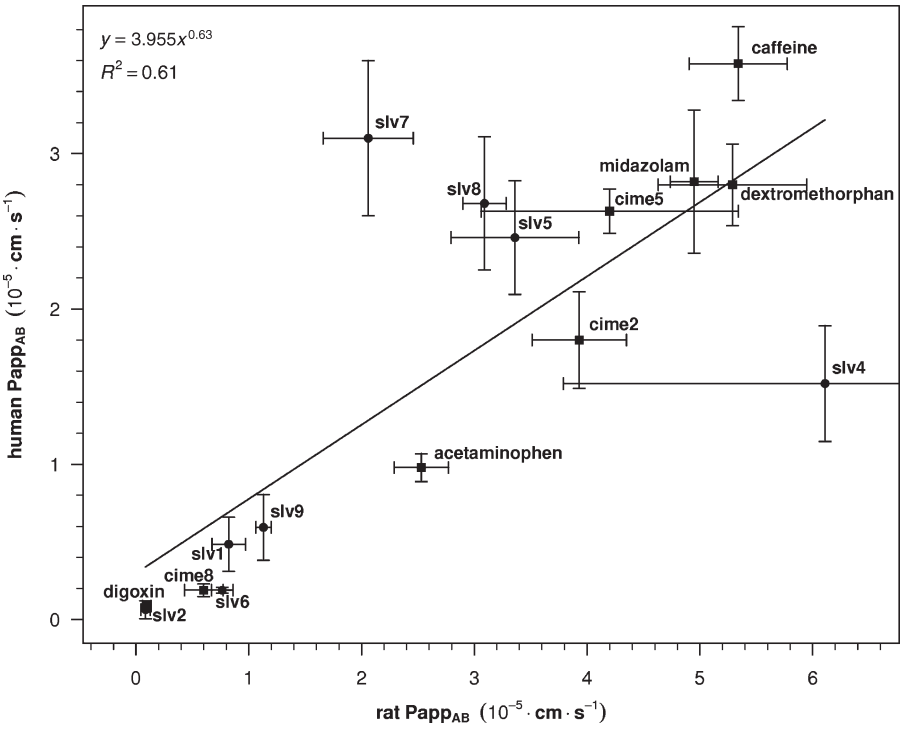

Figure 8. Species differences in blood−brain barrier transport. The full set correlated with an R^2 = 0.61. The R^2 increased to 0.91 when 11% of compounds (SLV4 and SLV7) were excluded from the correlation. Filled circles: SLV set. Filled squares: CIME set.

first of the two was observed to be potentially a substrate of an uptake transporter in the rat model (ER = 0.4) but not in the human cells (ER = 1.6).

The correlation between both species increased to 0.91 when two outliers (SLV4 and SLV7) were excluded from the relationship (Figure 8), and a trend of 2-fold higher permeability was noted in the rat model. These observations raise concerns that potential interspecies differences[31] may occur for some compounds and lead to a bias in the extrapolation of results obtained using the rat model to the human BBB.

■ DISCUSSION AND CONCLUSION

CNS drugs under development have a high failure rate.[32] Many of these failures may occur due to drugs not reaching the CNS target because of lack of BBB permeation. This is a major challenge that the pharmaceutical industry is facing and may be not only explained by complexities in extrapolating brain pharmacokinetics from animal to human but also due to the difficulty in developing a relevant screening tool in relation to BBB permeation. Until now, research flow schemes have mainly been based on an initial screening with a simple *in vitro* permeability model such as PAMPA or MDCK cells overexpressing human P-gp[14] and subsequent assessment of plasma and brain protein binding,[12,29,33] followed by *in vivo* experiments for the brain/plasma ratio determination in the animal species used for preclinical pharmacology studies. This current screening process may be considered as inappropriate if permeability is to be taken into account and does not allow interspecies extrapolation. It is essentially based on the assumption that brain penetration in human would be similar to that in animals. Even among the many *in vitro* BBB models described in literature only a few have demonstrated the presence of efflux transporters[25,30] and/or a low paracellular permeability as observed in the *in vivo* BBB. Most of the currently available *in vitro* BBB models used to mimic BBB permeability remain a mere approximation of the complex BBB structure composition and functions. In this investigational work, we report the *in vitro* primary rat and human cell-based BBB models as a more appropriate tool for early drug screening of CNS drug candidates.

First of all, membrane composition and functionalities of the *in vitro* cell-based BBB model have been highlighted, in addition to the fact that it is relatively easy to implement, standard and reproducible, and would allow a reduction in the use of animals. Similarly to the *in vitro* human cell-based BBB model, which was previously characterized[34] [mean P_{app} for 9 different batches from 9 different donors in three replicates at $2.69 \times 10^{-6} \pm 0.25 \times 10^{-6}$ cm s^{-1}], the *in vitro* primary rat cell-based BBB model exhibits a low paracellular permeability [mean P_{app} for 11 cell batches in three replicates at $3.28 \times 10^{-6} \pm 0.82 \times 10^{-6}$ cm s^{-1}] (Figure 2). These P_{app} values are 10-fold lower than those widely observed in currently available BBB models.[21−24] The results presented in Figure 1a,b indicate that the *in vitro* primary rat cell-based model adequately expressed specific tight junction proteins and more particularly claudin-5 proteins, which regulate the paracellular transport across the brain endothelial cell monolayer. Moreover, the *in vitro* primary rat cell-based BBB model is polarized, similarly to the *in vivo* BBB.

The mRNA expression for ABC transporters was measured. Transcript levels for the major efflux transporters such as abcb1 and abcg2 were evidenced. Those transporters are higly expressed and work in conjunction with limit distribution of compounds into the brain.[35,36] We did not detect mRNA for abcc6. While mRNA transcripts for abcc2, abcc4 and abcc5 in brain endothelial cells decreased in the presence of glial cells, mRNA transcripts for abcb1 in brain endothelial cells increased, suggesting the role of glial cell factors in the regulation of those

transporters as described elsewhere.[27] The mRNA expression for ABC transporters was measured, and functionality was confirmed. For instance, the efflux ratio for the P-gp substrate, vinblastine, is approximately 2.43 ± 0.48 (data for 10 batches of cells in three replicates: CV = 19.88%). In addition, compound SLV6, which showed an efflux ratio of about 15 in P-gp transfected MDCK cells,[11] presents an efflux ratio of 3.5 and 9.8 in *in vitro* rat and human cell-based BBB models (Table 1), respectively. This bidirectional transport of P-gp substrates suggests that transporters such as P-gp were functionally active and are located on the apical membrane of rat brain endothelial cells. Finally, Figure 3 shows that CNS and non-CNS compounds can be differentiated on the *in vitro* rat cell-based BBB model.

The BBB permeability of the twenty selected compounds was studied with the objectives of analyzing the *in vitro*/*in vivo* correlation in rats, taking into account multiple factors involved in brain exposure and interspecies differences between rat and human. When considering the *in vitro* BBB permeability studies in the present work, the mass balance study exceeded 80% of all compounds with the exception of three (SLV3, omeprazole, tolbutamide), which were therefore excluded from further data integration and statistical analyses.

The *in vitro* cell-based rat BBB model demonstrated a large dynamic range, with P_{app} values ranging from 0.85 to 61.13 × 10^{-6} cm s^{-1} for the selected compounds. In terms of support to chemical design in drug discovery, physicochemical properties of compounds such as PSA, MW, hydrogen acceptor bonding capacity and lipophilicity were observed to be inadequate for direct prediction with accuracy of their passage through the tight BBB. None of these characteristics correlated with the measured permeability (R^2 = 0.31; R^2 = 0.46; R^2 = 0.21 and R^2 = 0.018, respectively). Our findings are in agreement with certain literature data.[19,37] Apart from this first observation, a relationship by classification was found between drug physicochemical properties and *in vitro* BBB permeability: Figure 5 highlights a trend between MW, PSA, cLog P and *in vitro* P_{app}, which confirmed previous observations suggesting that PSA < 120 Å, MW < 450 and cLogP < 5 are required for brain-targeting drug candidates.[7,38]

To predict human pharmacokinetics from animal data remains a captivating challenge for researchers, and especially in discovery of CNS drugs because of the very specific target. Recent papers have shown a significant relationship between the brain/plasma protein binding and the brain/plasma exposure ratio.[7,8] This relationship is based on the assumption that the BBB permeability is mainly characterized by passive diffusion. Nevertheless, if the protein binding ratio reflects tissue affinity, BBB permeability has been well described as significantly impacting the rate and extent of brain penetration,[8] moreover when involving not only passive diffusion but also active uptake or efflux transports. When considering these factors all together, brain exposure may be estimated without direct tissue analysis but by simultaneous integration of plasma exposure, brain/plasma protein binding ratio, BBB permeability rate and efflux ratio (R^2: 0.67, $p = 2 \times 10^{-4}$) (Figure 7). This relationship would offer opportunities to significantly improve drug candidate selection via *in vitro* experiments, plasma and brain protein binding and *in vitro* cell-based BBB permeability studies. Moreover the *in vivo* plasma (only) pharmacokinetic experimentation phase would be considered similarly to a screening chart corresponding to a systemic target, thus reducing the number of studies and animals used in the research process. In addition, this relationship would also imply that the brain exposure in human can be predicted as soon as the first human plasma pharmacokinetics are available or based on prediction of human plasma exposure.

As part of the objective of studying interspecies differences in BBB permeability, the dynamic range of permeability between *in vitro* rat and human cell-based model was compared. One of the initial perspectives following the *in vitro* interspecies study would have been the use of the animal model as part of a research flow scheme instead of the human model, because this is obviously easier to implement and allows the pooling of brains from several animals, to therefore perform a significantly higher number of experiments per batch of cells and to integrate the interindividual variability. The visual inspection of Figure 8 reveals that there is a correlation between the two BBB models for the known CIME compounds (R^2 = 0.94). From the results obtained with the tested data set, Figure 8 illustrates a species mismatch for 11% (SLV4 and SLV7) of the tested compounds between *in vitro* rat and human cell-based BBB models. The differential permeability of both compounds may account for this species mismatch. Indeed, SLV4 exhibits 4-fold higher permeability in *in vitro* rat than in human cell-based BBB model, while SLV7 exhibits 1.5-fold higher permeability in human than in rat cell-based BBB model. SLV4 displays an efflux ratio (ER) of about 0.4 and 1 in rat and human, respectively. This ER of 0.4 suggests the involvement of influx transporter in *in vitro* rat cell-based BBB model. This difference in the permeability value in addition to the difference in the efflux ratio for SLV5 between rat (ER: 5.67) and human (ER: 0.9) may account for a negative correlation evidenced in Figure8 for SLV4, SLV5, SLV7 and SLV8.

In addition, permeability data from those conventional BBB assays (MDR1-MDCKII and Caco-2) were compared to data from our *in vitro* rat cell-based BBB models using SLV compounds and CIME substrates. A weak correlation was find on the one hand between Caco-2 cells and the *in vitro* rat cell-based BBB model (r^2: 0.48) and on the other hand between MDR1-MDCKII and the *in vitro* rat cell-based BBB model (r^2: 0.22). The differential correlation could be explained by the difference in membrane characteristics. For instance, it is well-known that MDR1-MDCKII cell membrane has lower ratios of phospholipid to cholesterol, unsaturated to saturated acyl chains, and phosphatidyl-choline to sphingomyelin than brain endothelial cells making this immortalized cell line a poor passive permeability model for BBB.[39] Moreover, our findings show difference in the expression level of transporter between Caco-2 cells and *in vitro* rat cell-based BBB model (data not shown). For instance, BCRP was more highly expressed in the *in vitro* rat cell-based BBB model than in Caco-2 cells. Conversely, MRP2 and MRP6 were highly expressed in Caco-2 cells while no expression was evidenced in the *in vitro* rat cell-based BBB model. Finally, the permeability comparison studies between different *in vitro* BBB systems which can be extended to different known substrates with high degree of interaction with known influx and/or influx transporters need to be specifically studied.

Nevertheless, even if a similar ranking of compounds was observed with the two models (rat and human cell-based BBB models), a trend of 2-fold higher permeability seemed to be evidenced in the rat versus the human model. This may indicate that early drug candidate screening (Hit to Lead—Lead optimization) could be done using the rat cell-based BBB, but on condition that potential differences in membrane composition and/or fluidity, and/or transporter expression/activity/affinity between species[31] are not dismissed. Therefore, both a full interspecies BBB membrane characterization and the use

of the human cell-based model at a later research phase (preclinical candidates) appear necessary for a fully integrated screening chart.

Collectively, our findings indicate that the *in vitro* primary rat and human cell-based blood−brain barrier models have been characterized as having relevant features of the *in vivo* blood−brain barrier and are suitable for discriminating CNS and non-CNS compounds. Considering that plasma pharmacokinetics are not CNS-specific, an optimized CNS drug discovery process may include physicochemical properties such as MW, PSA and cLogP, plasma and brain protein binding ratio, and the BBB permeability rate and efflux ratio. Standardization of the BBB animal and human cell-based models (validation of models with other species is currently ongoing) and their acceptance in the pharmaceutical industry has a potential to significantly decrease abortion of CNS drugs at later stages of drug development and would help to focus resources on promising compounds that are more likely to reach the target organ: the brain.

AUTHOR INFORMATION

Corresponding Author

*CEA, DSV, iBiTecS, Service de Pharmacologie et d'Immunoanalyse, Groupe Neuropharmacologie et Médicaments, 91191 Gif sur Yvette Cedex, France. Phone: 33 1 69 08 13 21. Fax: 33 1 69 08 59 07. E-mail: Aloïse.Mabondzo@cea.fr.

ACKNOWLEDGMENT

This work was supported by recurrent funds from the Commissariat à l'Energie Atomique (CEA). Discussion with, and suggestions from, Dr Praveen Balimane of Bristol-Myers Squibb Company are gratefully acknowledged. We wish to thank Elizabeth Mc Cann (Laboratoires Fournier S.A., 21121 Daix, France) for the copyediting work performed on this article.

REFERENCES

(1) Kola, I.; Landis, J. Can the pharmaceutical industry reduce attrition rates? *Nat Rev. Drug Discovery* **2004**, *3*, 711–5.

(2) Potschka, H. Targeting regulation of ABC efflux transporters in brain diseases: A novel therapeutic approach. *Pharmacol. Ther* **2010**, *125*, 118–27.

(3) Loscher, W.; Potschka, H. Drug resistance in brain diseases and the role of drug efflux transporters. *Nat. Rev. Neurosci.* **2005**, *6*, 591–602.

(4) Fischer, V.; Einolf, H. J.; Cohen, D. Efflux transporters and their clinical relevance. *Mini-Rev. Med. Chem.* **2005**, *5*, 183–95.

(5) Sun, H.; Dai, H.; Shaik, N.; Elmquist, W. F. Drug efflux transporters in the CNS. *Adv. Drug Delivery Rev* **2003**, *55*, 83–105.

(6) Taylor, E. M. The impact of efflux transporters in the brain on the development of drugs for CNS disorders. *Clin. Pharmacokinet.* **2002**, *41*, 81–92.

(7) Summerfield, S. G.; Read, K.; Begley, D. J.; Obradovic, T.; Hidalgo, I. J.; Coggon, S.; Lewis, A. V.; Porter, R. A.; Jeffrey, P. Central nervous system drug disposition: the relationship between in situ brain permeability and brain free fraction. *J. Pharmacol. Exp. Ther.* **2007**, *322*, 205–13.

(8) Hammarlund-Udenaes, M.; Friden, M.; Syvanen, S.; Gupta, A. On the rate and extent of drug delivery to the brain. *Pharm. Res.* **2008**, *25*, 1737–50.

(9) Liu, X.; Smith, B. J.; Chen, C.; Callegari, E.; Becker, S. L.; Chen, X.; Cianfrogna, J.; Doran, A. C.; Doran, S. D.; Gibbs, J. P.; Hosea, N.; Liu, J.; Nelson, F. R.; Szewc, M. A.; Van, D. J. Use of a physiologically based pharmacokinetic model to study the time to reach brain equilibrium: an experimental analysis of the role of blood-brain barrier permeability, plasma protein binding, and brain tissue binding. *J. Pharmacol. Exp. Ther.* **2005**, *313*, 1254–62.

(10) Fu, X. C.; Wang, G. P.; Shan, H. L.; Liang, W. Q.; Gao, J. Q. Predicting blood-brain barrier penetration from molecular weight and number of polar atoms. *Eur. J. Pharm. Biopharm.* **2008**, *70*, 462–66.

(11) Liu, X.; Tu, M.; Kelly, R. S.; Chen, C.; Smith, B. J. Development of a computational approach to predict blood-brain barrier permeability. *Drug Metab. Dispos.* **2004**, *32*, 132–39.

(12) Liu, X.; Smith, B. J.; Chen, C.; Callegari, E.; Becker, S. L.; Chen, X.; Cianfrogna, J.; Doran, A. C.; Doran, S. D.; Gibbs, J. P.; Hosea, N.; Liu, J.; Nelson, F. R.; Szewc, M. A.; Van, D. J. Use of a physiologically based pharmacokinetic model to study the time to reach brain equilibrium: an experimental analysis of the role of blood-brain barrier permeability, plasma protein binding, and brain tissue binding. *J. Pharmacol. Exp. Ther.* **2005**, *313*, 1254–62.

(13) Wan, H.; Ahman, M.; Holmen, A. G. Relationship between brain tissue partitioning and microemulsion retention factors of CNS drugs. *J. Med. Chem.* **2009**, *52*, 1693–700.

(14) Balimane, P. V.; Han, Y. H.; Chong, S. Current industrial practices of assessing permeability and P-glycoprotein interaction. *AAPS J.* **2006**, *8*, E1–13.

(15) Marino, A. M.; Yarde, M.; Patel, H.; Chong, S.; Balimane, P. V. Validation of the 96 well Caco-2 cell culture model for high throughput permeability assessment of discovery compounds. *Int. J. Pharm.* **2005**, *297*, 235–41.

(16) Liu, Y.; Zeng, S. Advances in the MDCK-MDR1 cell model and its applications to screen drug permeability. *Yaoxue Xuebao* **2008**, *43*, 559–64.

(17) Tang, F.; Horie, K.; Borchardt, R. T. Are MDCK cells transfected with the human MRP2 gene a good model of the human intestinal mucosa? *Pharm Res.* **2002**, *19*, 773–79.

(18) Summerfield, S. G.; Lucas, A. J.; Porter, R. A.; Jeffrey, P.; Gunn, R. N.; Read, K. R.; Stevens, A. J.; Metcalf, A. C.; Osuna, M. C.; Kilford, P. J.; Passchier, J.; Ruffo, A. D. Toward an improved prediction of human in vivo brain penetration. *Xenobiotica* **2008**, *38*, 1518–35.

(19) Tanaka, H.; Mizojiri, K. Drug-protein binding and blood-brain barrier permeability. *J. Pharmacol. Exp. Ther.* **1999**, *288*, 912–8.

(20) Dagenais, C.; Avdeef, A.; Tsinman, O.; Dudley, A.; Beliveau, R. P-glycoprotein deficient mouse in situ blood-brain barrier permeability and its prediction using an in combo PAMPA model. *Eur. J. Pharm. Sci.* **2009**, *38*, 121–37.

(21) Cucullo, L.; Couraud, P. O.; Weksler, B.; Romero, I. A.; Hossain, M.; Rapp, E.; Janigro, D. Immortalized human brain endothelial cells and flow-based vascular modeling: a marriage of convenience for rational neurovascular studies. *J. Cereb. Blood Flow Metab.* **2008**, *28*, 312–28.

(22) Deli, M. A.; Abraham, C. S.; Kataoka, Y.; Niwa, M. Permeability studies on in vitro blood-brain barrier models: physiology, pathology, and pharmacology. *Cell. Mol. Neurobiol.* **2005**, *25*, 59–127.

(23) Weksler, B. B.; Subileau, E. A.; Perriere, N.; Charneau, P.; Holloway, K.; Leveque, M.; Tricoire-Leignel, H.; Nicotra, A.; Bourdoulous, S.; Turowski, P.; Male, D. K.; Roux, F.; Greenwood, J.; Romero, I. A.; Couraud, P. O. Blood-brain barrier-specific properties of a human adult brain endothelial cell line. *FASEB J.* **2005**, *19*, 1872–74.

(24) Zhang, Y.; Li, C. S.; Ye, Y.; Johnson, K.; Poe, J.; Johnson, S.; Bobrowski, W.; Garrido, R.; Madhu, C. Porcine brain microvessel endothelial cells as an in vitro model to predict in vivo blood-brain barrier permeability. *Drug Metab. Dispos.* **2006**, *34*, 1935–43.

(25) Josserand, V.; Pelerin, H.; de, B. B.; Jego, B.; Kuhnast, B.; Hinnen, F.; Duconge, F.; Boisgard, R.; Beuvon, F.; Chassoux, F.; Dumas-Duport, C.; Ezan, E.; Dolle, F.; Mabondzo, A.; Tavitian, B. Evaluation of drug penetration into the brain: a double study by in vivo imaging with positron emission tomography and using an in vitro model of the human blood-brain barrier. *J. Pharmacol. Exp. Ther.* **2006**, *316*, 79–86.

(26) Hembury, A.; Mabondzo, A. Endothelin-1 reduces p-glycoprotein transport activity in an in vitro model of human adult blood-brain barrier. *Cell. Mol. Neurobiol.* **2008**, *28*, 915–21.

(27) Megard, I.; Garrigues, A.; Orlowski, S.; Jorajuria, S.; Clayette, P.; Ezan, E.; Mabondzo, A. A co-culture-based model of human blood-brain

barrier: application to active transport of indinavir and in vivo-in vitro correlation. *Brain Res.* **2002**, *927*, 153–67.

(28) Tanaka, H.; Mizojiri, K. Drug-protein binding and blood-brain permeability. *Pharmacol. Exp Ther* **1999**, *288*, 912–18.

(29) Jeffrey, P.; Summerfield, S. G. Challenges for blood-brain barrier (BBB) screening. *Xenobiotica* **2007**, *37*, 1135–51.

(30) Bousquet, L.; Roucairol, C.; Hembury, A.; Nevers, M. C.; Creminon, C.; Farinotti, R.; Mabondzo, A. Comparison of ABC transporter modulation by atazanavir in lymphocytes and human brain endothelial cells: ABC transporters are involved in the atazanavir-limited passage across an in vitro human model of the blood-brain barrier. *AIDS Res. Hum. Retroviruses* **2008**, *24*, 1147–54.

(31) Syvanen, S.; Lindhe, O.; Palner, M.; Kornum, B. R.; Rahman, O.; Langstrom, B.; Knudsen, G. M.; Hammarlund-Udenaes, M. Species differences in blood-brain barrier transport of three positron emission tomography radioligands with emphasis on P-glycoprotein transport. *Drug Metab. Dispos.* **2009**, *37*, 635–43.

(32) Hurko, O.; Ryan, J. L. Translational research in central nervous system drug discovery. *NeuroRx* **2005**, *2*, 671–82.

(33) Read, K.; Braggio, S. Assessing brain free fraction in early drug discovery. *Expert Opin. Rev.* **2010**, *6*, 1–8.

(34) Mabondzo, A.; Bottlaender, M.; Guyot, A.-C.; Tsaouin, K.; Deverre, J. R.; Balimane, P. V. Validation of In Vitro Cell-Based Human Blood-Brain Barrier Model Using Clinical Positron Emission Tomography Radioligands To Predict In Vivo Human Brain Penetration. *Mol. Pharmaceutics* **2010**, *7* (5), 1805–15.

(35) Cisternino, S; Bourasset, M. C.; Roux, F; Scherrmann, J. M. Expression, up-regulation, and transport activity of the multidrug-resistance protein Abcg2 at the mouse blood-brain barrier. *Cancer Res.* **2004**, *64*, 3296–301.

(36) De Vries, N. A.; Zhao, J.; Kroon, E.; Buckle, T.; Beijnen, J. H.; Van Telligen, O. P-glycoprotein and breast cancer resistance protein: two dominant transporyters working together in limiting the brain penetration of topotecan. *Clin. Cancer Res.* **2007**, *13*, 6440–9.

(37) Wong, D. F.; Pomper, M. G. Predicting the success of a radiopharmaceutical for in vivo imaging of central nervous system neuroreceptor systems. *Mol. Imaging Biol.* **2003**, *5*, 350–62.

(38) Hitchcock, S. A.; Pennington, L. D. Strcuture-brain exposure relationships. *J. Med. Chem.* **2006**, *49*, 7559–83.

(39) Li, D.; Kerns, E. D.; Bezar, I. F.; Petusky, S. L.; Huang, Y. *J. Pharm. Sci.* **2009**, *98*, 1980–91.